Chapter 5

Ground based observations of comets in the optical wavelengths range

5.1 Optical longslit spectroscopy

Figure 5.1 illustrates the principle of optical longslit spectroscopy using a focal reducer-type instrument. It is easily understood, following the figure from left to right. The object is observed through a slit which is positioned in the focal plane. This results in a spatial intensity profile of the object along the orientation of the slit. A collimator (not shown in the figure) generates a parallel light beam. This light beam falls on a dispersive element, usually a grism, which creates a spectrum for each point on the spatial profile, which is registered by the CCD. The result is a spatially resolved spectrum of the object as seen on the right of figure 5.1.
The advantage of longslit spectroscopy is the ability to study the spatial distribution of emission features. The choice of grating and slit setup allows to address a wide range of observations, from high spatial resolution spectroscopy to study the near nucleus region to high dispersion spectroscopy to study in detail the band structure of emission systems.
For this work the slit was usually centered on the optocenter of the coma. With different slit orientations asymmetries in the cometary coma can be addressed. By offsetting the slit position the distribution within the coma can be studied. Some observations have been obtained with the slit offset in the tailward direction. This allows to study the composition of the tail directly.

5.2 Spectra of comets in the optical wavelengths range

For this work a brief introduction of the mechanism of fluorescence will be given and the the typical spectrum of a comet in the optical wavelength range will be discussed. For other emission mechanisms, like collision excitation and prompt emission, the reader is referred to the literature (for example the book by Huebner [1990], the articles by Crovisier and Encrenaz [1983]; Crovisier [1987] or the review by Rauer [2002]).

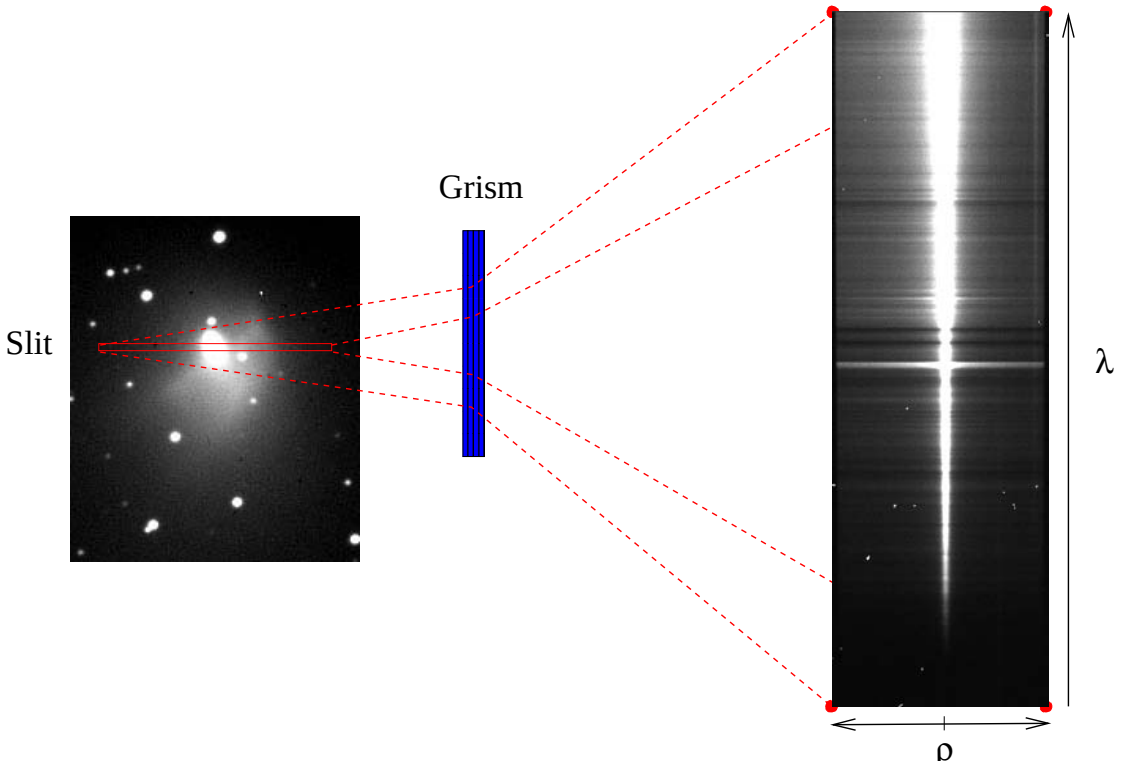

Figure 5.1: Principle of the optical longslit spectroscopy

Emissions observed in the optical wavelength range are produced by fluorescence. Fluorescence means the absorption of a solar photon of appropriate wavelength by a molecule leading to an electronically and/or vibrational excited state. This is followed by spontaneous emission of one or more photons in a single or multi-step decay process which may or may not leave the molecule in the ground state. If the emitted photon has the same wavelength as the absorbed photon this process is called resonance fluorescence.
The fluorescence efficiency g is defined as the number of photons emitted per second and per molecule within a given electronic-vibrational band. As long as the excitation is simple fluorescence from the ground state of a molecule and nearly the entire population of the molecule considered is in the ground state, it is sufficient to calculate the absorption rate of solar photons to the upper level and multiply by the appropriate branching ratio for the transition

$$g = B_{ik}\rho_{\nu_{ik}} \frac{A_{kj}}{\sum\limits_{j<k} A_{kj}} \tag{5.1}$$

A_{kj}, B_{ik}	Einstein coefficients
$\rho_{\nu_{ik}}$	solar radiation density at the frequency ν_{ik} and at r_h=1 AU

In general the situation is much more complex. The excitation is not simple resonance fluorescence and a significant population is not in the ground state, but distributed over

one or more levels. The way to solve this problem is to assume that the population is in radiative equilibrium. In this case a set of balance equations can be set up for each level, where the rate of transition out of the level is set equal to the rate of transitions into the level (for details see Huebner [1990]). Appendix B contains a table with the 'g-factor' for the emissions of C_2, C_3 and NH_2 used for this work. For more details on the evaluation of these values the reader is referred to the references given in table B.1.
The situation is complicated by the fact that the solar spectrum contains strong absorption lines, known as Fraunhofer lines. Any calculation of the fluorescence efficiency factors must take these lines into account. Their wavelengths in a comet internal reference system can be shifted by the Doppler effect, since the heliocentric velocity of a comet can reach several tens of kilometer per second. This is known as the Swings effect [Swings *et al.*, 1941]. In the optical wavelengths range this effect is important for the CN emission at 3880 Å. Table B.3 in Appendix B shows the values used in this work based on model calculations done by Schleicher [1983] in his PhD thesis. There is a second effect leading to observed differences in the molecular bands in the sunward and tailward direction. The radial expansion velocity of the coma introduces a different shift sunward and tailward. This differential Swings effect is often referred to as the Greenstein effect [Greenstein, 1958].
Figure 5.2 shows a typical spectrum of Hale-Bopp obtained in the longterm monitoring program after data reduction. The blue end of the spectrum is dominated by the $B^2\Sigma^+$–$X^2\Sigma^+$ violet system of CN at 3880 Å marked by the band sequence CN(0-0) and CN(1-0). The spectral resolution does not allow to resolve the band systems. The $\tilde{A}^1\Pi_u$–$\tilde{X}^1\Sigma_g^+$ system of C_3 at 4040 Å is simply marked as C_3. This band system is at least partly resolved. Details on the fluorescence spectrum of C_3 can be found in Rousselot *et al.* [2001]. The CH band system at 4300 Å is only just detectable. At longer wavelengths follows the $d^3\Pi_g$–$a^3\Pi_u$ Swan system of C_2 at 5160 Å. The C_2 band sequences are denoted by giving the change in the vibrational level Δv=1,0,-1,-2. It should be noted that fluorescence emission leaves the C_2 molecule in the excited $a^3\Pi_u$ state. The fluorescence spectrum of C_2 has been recently studied by Rousselot *et al.* [2000]. The red end of the observed spectrum shows the $\tilde{A}^2A_1$–$\tilde{X}^2B_1$ system of NH_2 at 5700 Å. It is interesting to note that only transitions from levels with even upper vibrational quantum numbers to the ground state are visible. Transitions from levels with odd upper vibrational quantum numbers are much weaker. This was reported already by Rauer *et al.* [1997] based on the preperihelion observations of comet Hale-Bopp. Recent studies on the emission features of NH_2 by Glinski *et al.* [2001] have discussed this problem in detail and present an excitation model reproducing the evaluation of the observed emissions with heliocentric distance.

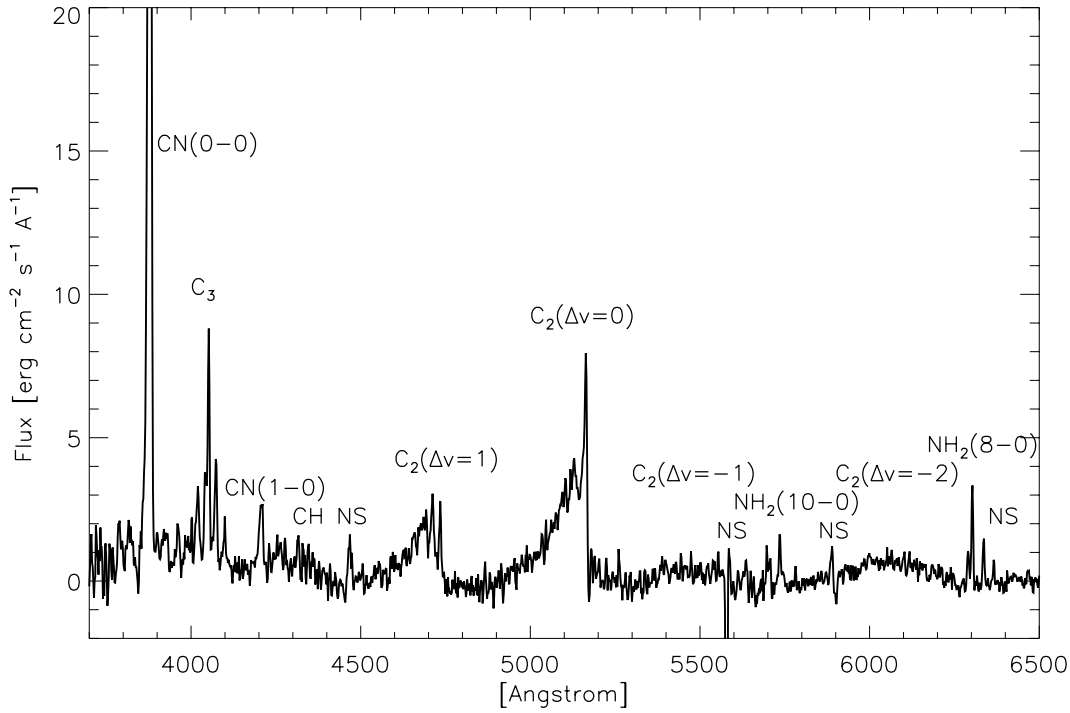

Figure 5.2: Cut through a reduced spectrum at 80000 km projected nucleocentric distance sunward. The spectrum was obtained on December 19, 1997 (r_h = 3.8 AU, 1200 s exposure time). The underlying continuum level caused by solar light scattered on dust particles has been subtracted. The main gas emission bands are marked. Residuals of night sky emissions are indicated (NS).

For this work four of the radicals observed in the optical have been studied: CN, NH_2, C_2 and C_3. While the first two have been studied only using the Haser model and the detailed study is part of the paper by Rauer *et al.* [2002], the focus of this work was on the latter two radicals, C_2 and C_3. For this reason only a brief overview of the formation chemistry of CN and NH_2 is given here. The formation chemistry of the C_2 and C_3 radical is described in much greater detail in the sections 11.1 and 11.2 in chapter V.

5.3 Chemistry of the CN parent molecules

It is widely accepted that hydrogen cyanide HCN is the dominant source of CN. The photo dissociation of HCN was studied in the laboratory for example by West [1975] and Jackson [1976]

$$\mathrm{HCN} \quad \longrightarrow \quad \mathrm{CN} + \mathrm{H}$$

The excess energy for this process is 3.82 eV.
A second proposed source of CN is cyanoacetylene HC_3N. As shown by Halpern *et al.* [1988] there are two possible dissociation reactions

$$\begin{aligned} \mathrm{HC_3N} \quad &\longrightarrow \quad \mathrm{C_2H} + \mathrm{CN} \\ &\longrightarrow \quad \mathrm{H} + \mathrm{C_3N} \end{aligned}$$

The second reaction is immediately followed by

$$\mathrm{C_3N} \quad \longrightarrow \quad \mathrm{C_2} + \mathrm{CN}$$

The dissociation of HC_3N via C_3N is the main channel as has not only been shown by Halpern, but before already by Job and King [1966] and by Seki [1985].
Another molecule which constantly resurfaces in the discussion of possible CN parents is C_2N_2. This was already proposed by Swings and Haser [1956]. The molecule simply dissociates to two CN radicals [Conners *et al.*, 1974].

$$\mathrm{C_2N_2} \quad \longrightarrow \quad \mathrm{CN} + \mathrm{CN}$$

5.4 Chemistry of the NH_2 parent molecules

The main parent of NH_2 is ammonia NH_3. The photodissociation of this molecule has been studied by e.g. McNesby and Okabe [1965]

$$\begin{aligned} NH_3 &\longrightarrow NH + H_2 \\ &\longrightarrow NH_2 + H \end{aligned}$$

For the solar spectrum the second process is most dominant.
Krasnopolsky and Tkachuk [1991] considered two further possible parent molecules: methylamine CH_3NH_2 and hydrazine N_2H_4.

$$\begin{aligned} CH_3NH_2 &\longrightarrow CH_3 + NH_2 \\ N_2H_4 &\longrightarrow NH_2 + NH_2 \end{aligned}$$

But their analysis of the VEGA observation of comet Halley pointed already strongly toward NH_3 as the dominant parent. This was confirmed by Kawakita and Watanabe for comet Hyakutake [Kawakita and Watanabe, 1998].